

Monitoring severe aquifer-system compaction and land subsidence in Taiwan using multiple sensors: Yunlin, the southern Choushui River Alluvial Fan

Wei-Chia Hung · Cheinway Hwang ·
Chung-Pai Chang · Jiun-Yee Yen · Chih-Hsi Liu ·
Wan-Huei Yang

Received: 15 June 2008 / Accepted: 26 February 2009 / Published online: 18 March 2009
© Springer-Verlag 2009

Abstract During 1992–2007, excessive pumping of groundwater caused large-scale aquifer-system compaction and land subsidence in the Choushui River Alluvial Fan, especially in the area of Yunlin county. The subsidence impedes surface-water runoff and endangers the operation of Taiwan High Speed Rail. Leveling, Global Positioning System (GPS), multi-level compaction monitoring well, and Differential Interferometric Synthetic Aperture Radar (DInSAR) are used to study the extent of subsidence in Yunlin and its mechanism. These sensors complement each other in spatial and temporal resolutions. A leveling network totaling 434 km in length was deployed to derive subsidence at every 1.5 km along the routes, and the result is accurate to few mm and shows a basin-like subsidence pattern centering at Tuku Township. Four multi-level compaction monitoring wells, co-located with GPS pillars,

detect compactions at different depths, showing that the aquifer-system compaction (the cause of subsidence) occurs mostly below depths >200 m, where reduction of groundwater pumping is most needed. The vertical displacements from GPS and leveling agree to within 1 cm, and are larger than the cumulative compaction detected by the compaction-monitoring wells, suggesting that compaction also occurs below 300 m (the depth of the wells). The vertical displacements derived using DInSAR and 8 ENVISAT SAR images agree with the leveling result to 1–2 cm.

Keywords Choushui River Alluvial Fan · DInSAR · GPS · Leveling · Monitoring well

Introduction

Growing population leads to great water demands. When there is insufficient surface water to meet the demand, groundwater is explored. Land subsidence due to withdrawal of groundwater has become a worldwide problem (Galloway et al. 1999). It results in flooding, poor drainage, sea-water intrusion, settling of buildings and civil infrastructures (Hasanuddin et al. 2001). Subsidence features in one region can be quite different from other regions because of the high variability of geologic-materials and complex depositional processes in different regions. Therefore, regional study is important, and the reliability of such a study depends on field investigations and in situ monitoring programs. Examples of regional subsidence studies can be found in Pietro et al. (2007) and Marfai and King (2007).

Taiwan ranks 15th in the world in population density (639 persons per km², including mountainous areas) (United Nations World Prospects Report, 2004 revision). Due to economic development in Taiwan, there is a

W.-C. Hung · C.-H. Liu
Energy and Resource Laboratories, Industrial Technology
Research Institute, Bldg. 24, 195 Sec. 4, Chung Hsing Rd.,
Chutung, Hsinchu 310, Taiwan

W.-C. Hung · C. Hwang (✉)
Department of Civil Engineering,
National Chiao Tung University,
1001 Ta Hsueh Road, Hsinchu 300, Taiwan
e-mail: cheinway@mail.nctu.edu.tw; cheinway@gmail.com
URL: <http://space.cv.nctu.edu.tw>

C.-P. Chang · J.-Y. Yen · W.-H. Yang
Department of Earth Sciences, Institute of Geophysics,
National Central University, No. 300, Jhongda Rd.,
Jhongli City, Taoyuan 320, Taiwan

J.-Y. Yen
Institute of Earth Sciences,
National Hualien University of Education,
No. 123, Huasi Rd., Hualien 970, Taiwan

growing demand for water resources, which are relatively scarce if the population density is taken into account. Currently, use of groundwater is common in the coastal zones of Taiwan and this has led to land subsidence. According to Hung (2007), in 2001, the total area with a subsidence rate >3 cm/year was 1,600 km². Since 2001, the Taiwan government has attempted to mitigate subsidence through such measures as restriction of groundwater pumping, forestation, and constructing dams to reduce subsidence. As such, the area with a subsidence rate >3 cm/year was reduced to 803 km² in 2007, 97% of which occurred in the Choshui River Alluvial Fan (CRAF).

CRAF is the most important agricultural area in west-central Taiwan, with elevations ranging from 0 to 100 m. CRAF covers a total area of 2,000 km² and is bounded by Wu River (north), Pekang Creek (south), Douliu Mound (east) and Taiwan Strait (west). Figure 1 shows the geographical location of CRAF, which is centered at 24°N and 120.5°E.

Choshui River is the longest river in Taiwan. The sediments in CRAF originate from rock formations in the upstream watershed of Choshui River, including slate, metamorphic quartzite, shale, sandstone, and mudstone (Fig. 2). Sediment loads composed of weathered rock fragments of different sizes gradually settled on the riverbed, flood plain, and seabed to form CRAF. The head of CRAF contains mainly gravel and coarse sand, and the toe is a delta covered by fine sand. Because the proximal fan reaches of Choshui River are wide and infiltrative, surface water on the proximal fan readily infiltrates the subsurface and recharges the aquifers.

The thickness of the sediments in CRAF ranges from 750 to 3,000 m (Lin et al. 1992). Due to frequent flooding and channel migration of the Choshui River, the flood-plain deposits contain inter-bedded or lens-structured clay, fine sand, medium fine sand, coarse sand, and gravel layers. Figure 3 shows the layering of these heterogeneous deposits along two profiles in Yunlin County (see below)

Fig. 1 Geographical location of Choshui River Alluvial Fan. Inserted is a map showing Yunlin in Taiwan

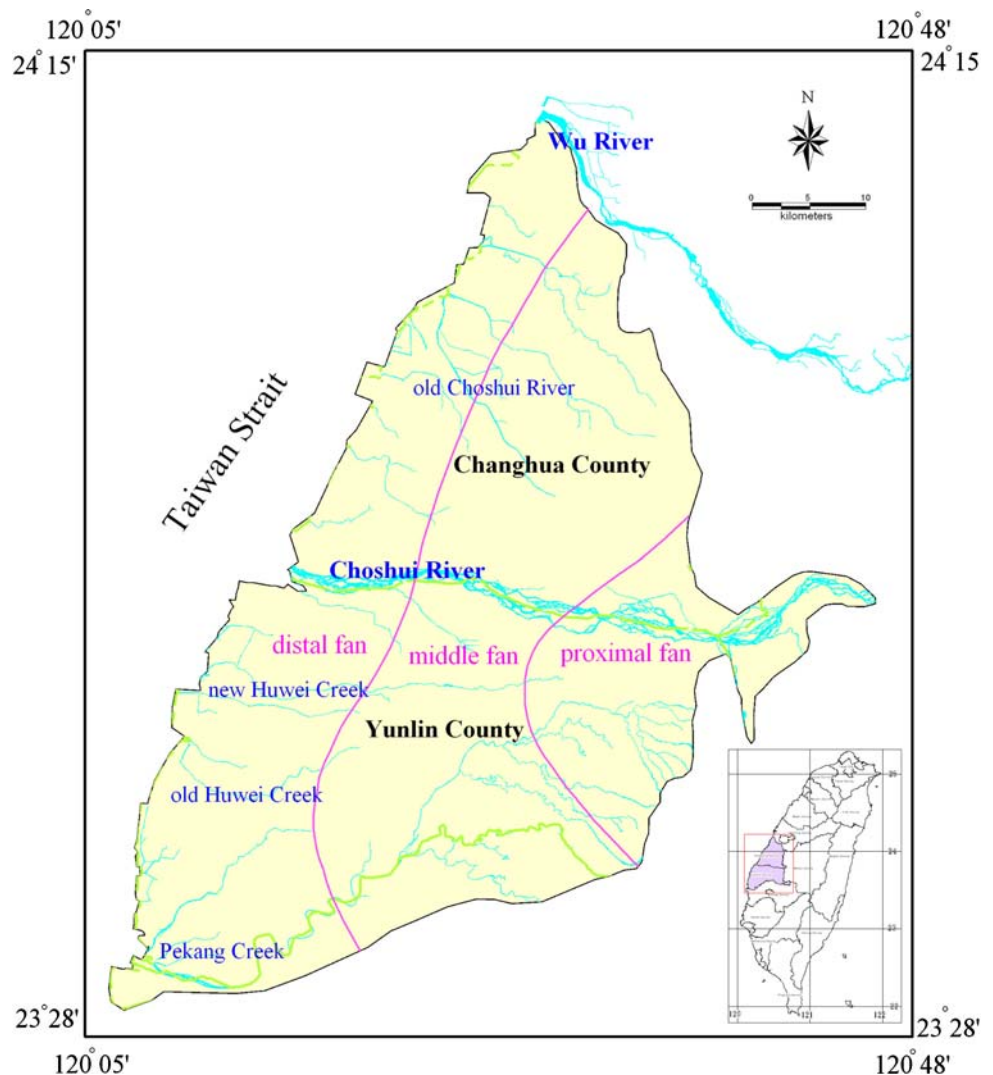
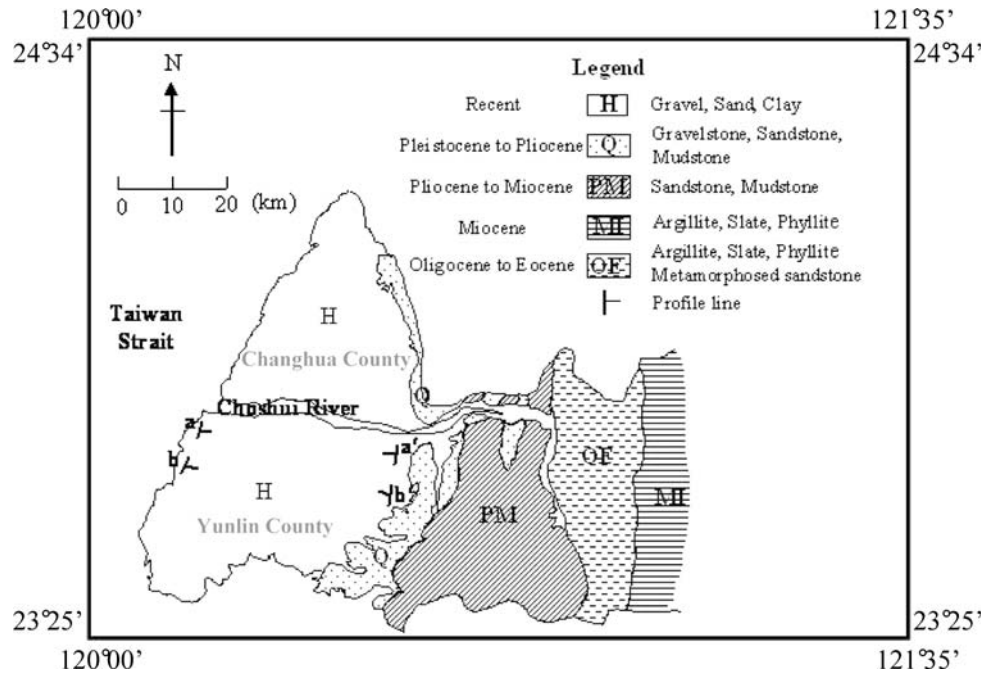


Fig. 2 Geological settings of Choshui River Alluvial Fan (modified from Central Geological Survey of Taiwan, <http://www.moeacgs.gov.tw/>)



from land surface to a depth of 300 m. The studies of rock properties, dating, fossil, and permeability suggest that the inter-bedded deposits create four interlayering aquifers and aquitards in the CRAF.

Figure 4 depicts the conceptual hydrogeology model of the CRAF. The aquitards are formed with mostly clayey soils and play a significant role in land subsidence. The four aquifers in the head of the fan are essentially connected (Liu et al. 2001). Near the head of the fan the aquifers are mainly composed of gravel and coarse sand, which become finer towards the center and the toe of the CRAF. In certain areas, these aquifers contain two or three interbedded clayey layers. These clayey layers are loosely scattered in the aquifers, and their extents and thickness are negligible compared to the four major aquitards (CGS 1999; Tyan et al. 1996). Hence, these clayey layers can be treated as clay lens structures within those aquifers, and are susceptible to compaction caused by groundwater pumping in these aquifers.

The southern part of the CRAF overlaps largely with Yunlin County. Due to the lack of surface water and the flat terrain that prohibit dam construction, the water for civilian and agricultural use in Yunlin comes largely from groundwater and the Chi-Chi Reservoir in the upstream reaches of the Choshui River. According to the statistics of the Water Resource Agency of Taiwan, the extracted groundwater in Yunlin is 94 metric tons a day, totaling 305 million tons a year. Figure 5 shows the distribution of groundwater pumping wells, with the total number exceeding 100,000. These wells are largely located in the middle fan and distal fan sections of the CRAF, and are

situated over a zone in the aquifer system composed of materials that are highly compressible. Withdrawing groundwater without recharge here will decrease the water level and consequently reduce the porous pressure and increase the effective stress, inevitably leading to aquifer-system compaction and land subsidence. The Taiwan High Speed Rail (THSR) passes through Yunlin, where subsidence poses a serious threat to its operation (Hwang et al. 2008).

Synergy of monitoring sensors

Earlier studies such as Hung (2007) show that the spatial-temporal characteristics of subsidence in Yunlin are complicated. To better understand the behavior of subsidence here, a multi-sensor monitoring system is envisioned. The general considerations in choosing monitoring sensors are as follows: (1) high spatial sampling density, (2) good measurement accuracy, and (3) high measurement frequency. The choice of sensors is very often dictated by available funds, which are the main limitation when a regional monitoring project is to be carried out. Under the constraint of funding, in this paper we decided to use leveling, Global Positioning System (GPS), multi-level compaction monitoring wells, and Differential Interferometric Synthetic Aperture Radar (DInSAR). A short summary of these sensors in terms of their advantages and disadvantages is given below.

- (1) *Leveling*: Leveling determines the height difference using backsight and foresight readings from leveling

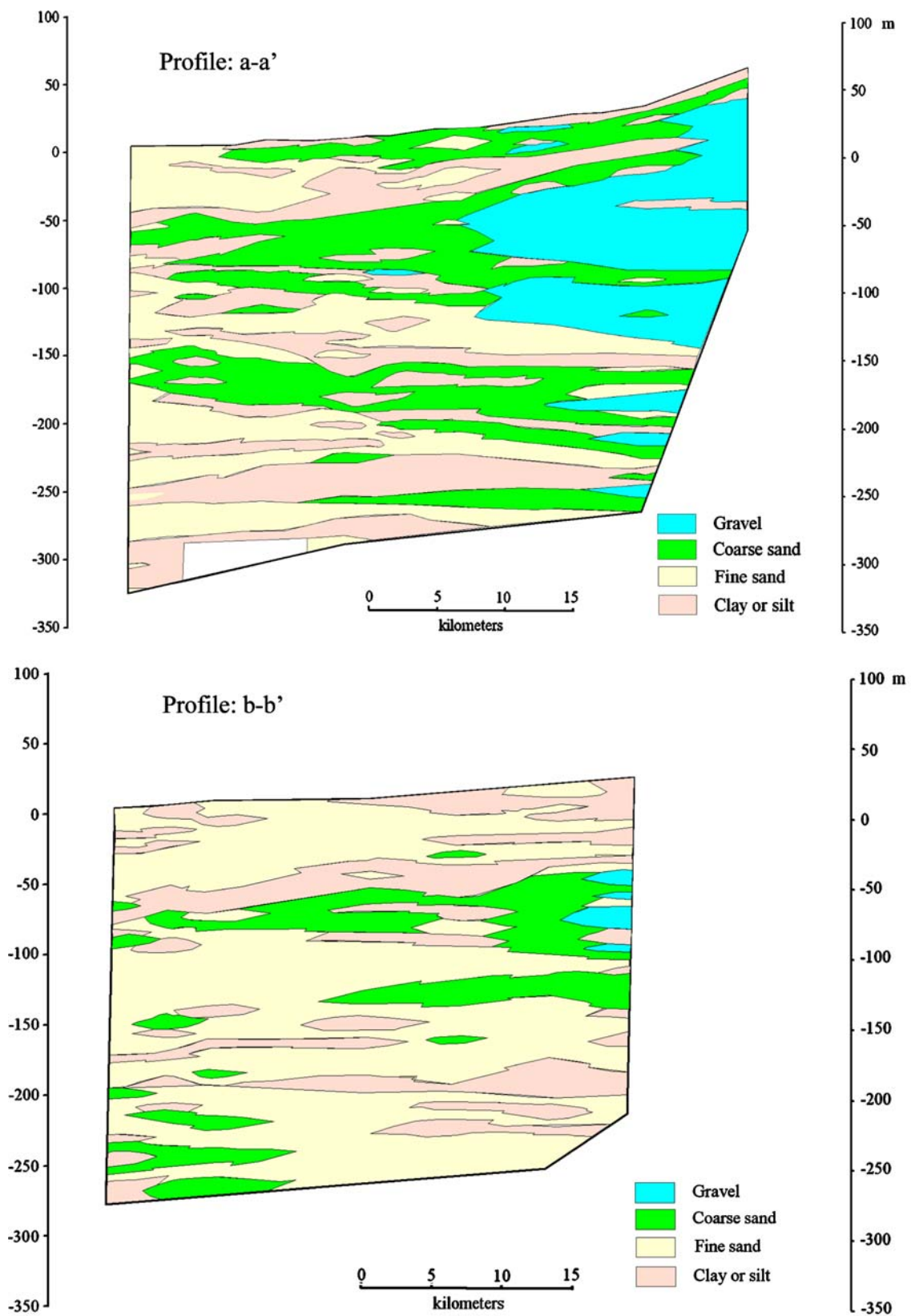


Fig. 3 Cross sections showing distributions of unconsolidated deposits along profiles a-a' and b-b' (see Fig. 2). The western ends of the profiles are the Taiwan Strait

Fig. 4 Distribution of aquifers and aquitards along profile a-a' (Fig. 3)

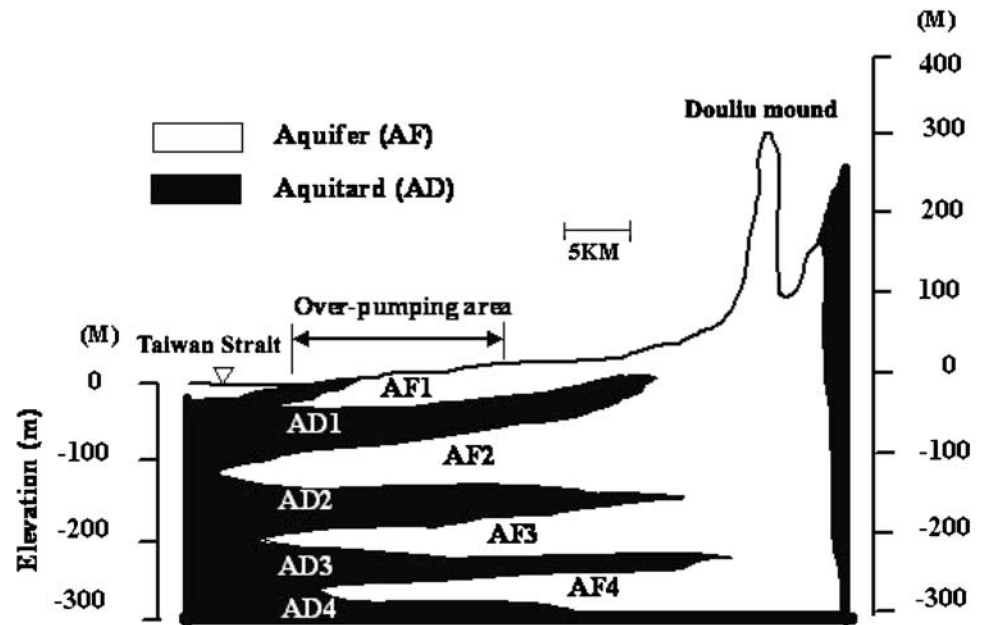
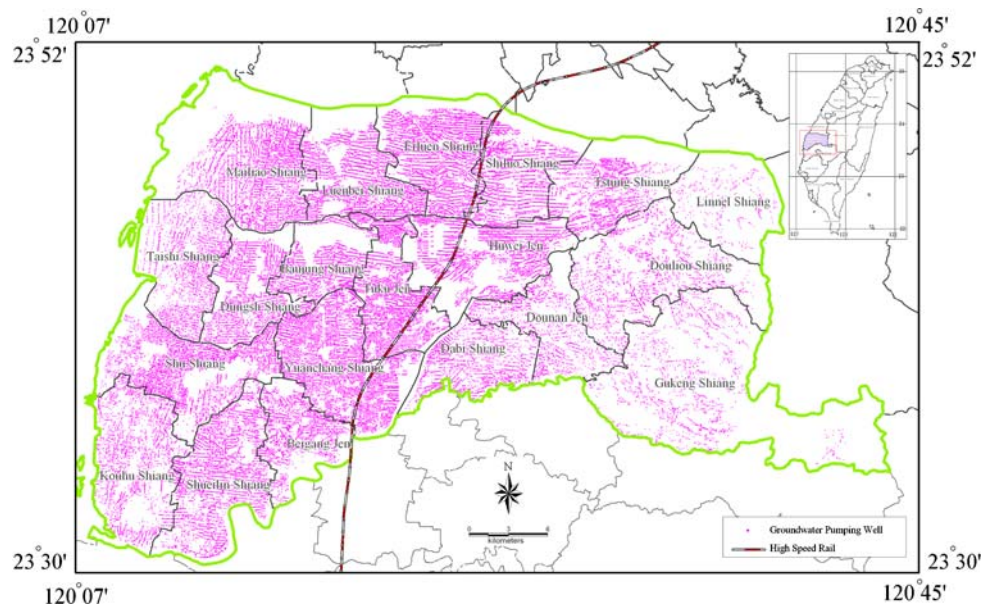


Fig. 5 Distribution of groundwater pumping wells in Yunlin



rods, and is commonly used in height change monitoring. The advantage of leveling is high accuracy (several mm), and its disadvantage is being slow and costly compared to GPS.

- (2) *GPS*: GPS determines three-dimensional point positions. The vertical accuracy can be better than 1 cm if the GPS signals are not blocked and the GPS record length is sufficiently long. The advantage is its good mobility and speedy survey operation, and the disadvantage is its lower accuracy (about 1 cm) in the vertical component compared to that of leveling.
- (3) *Multi-level compaction monitoring well*: The device measures compaction of the aquifer system at different depths and is a good tool for understanding the

- (4) *DInSAR*: DInSAR uses radar images of different times to measure the line-of-sight component of surface displacement. It can monitor vertical displacement at a favorable spatial resolution and accuracy (about 1–2 cm), which is the advantage. The disadvantage is that DInSAR is affected by various errors that may reduce its accuracy (see Section “Spatially detailed monitoring of subsidence by differential radar interferometry”).

Table 1 summarizes the spatial resolutions, measurement frequencies, and measurement (vertical) accuracies of these sensors. Used together, these sensors complement each other in terms of their spatial and temporal resolutions. With a good spatial correlation and proper environmental corrections, DInSAR with ENVISAT images line-of-sight displacements are accurate to a few cm with a 25 m spatial resolution at a time scale equivalent to the satellite's 35-day orbital cycle (Hooper et al. 2004). At a continuous GPS station, the accuracy of vertical changes can be determined to 1 cm on a daily solution. Using a high-precision level and good correction models, leveling can deliver point-wise vertical displacements accurate to few mm along leveling routes. Figure 6 shows the leveling routes, monitoring wells, and continuous GPS stations deployed in this study.

Monitoring of subsidence by leveling

Our leveling network covers a zone bounded by Choshui River, Pekang Creek, Linai Township, and Taiwan Strait. The benchmarks in the net were established by the Water Resource Agency of Taiwan. There are 53 main routes in

the network, forming 13 loops. Covering an area of 1,087 km², the network has a total length 434 km and a density of one benchmark every 1.5 km. A large portion of the leveling network is deployed in a zone west of the Sun Yat-Sen Highway, where the major subsidence has occurred (Hung 2007). The reference benchmark, WR12 (Fig. 6), is considered stable and its elevation is fixed when least-squares adjusting the observed differential heights in the network. Six leveling surveys were carried out in 2000, 2002, 2003, 2005, 2006, and 2007.

A Trimble Dini 11 digital level was used to collect differential heights. This level was calibrated by the Center for Measurement Standards of Taiwan before the leveling surveys. The specifications of our leveling survey demand that any loop misclosure be below $3\text{ mm}\sqrt{K}$, where K is the distance between two neighboring benchmarks in km. Errors due to collimation, earth's curvature, and atmospheric refraction were corrected. Because the terrain of the CRAF is flat and the elevation is small (0–100 m), orthometric correction is mostly less than 0.1 mm; hence, it was not applied to the differential heights (Hwang and Hsiao 2003). Also, no temperature and reading corrections were needed because of the use of INVAR leveling rods. The corrected differential heights were first screened for

Table 1 Multi-sensor comparison table

	Leveling	Continuous GPS	Monitoring well	DInSAR
Spatial resolution	1.5–2 km	10–15 km	5–10 km	25 m
Measurement frequency	1 year	1 day	1 month	35 day
Measurement (vertical) accuracy	0.5–1 cm	0.5–1 cm	0.1–0.5 cm	2 cm

Fig. 6 Distributions of leveling routes, monitoring wells and GPS stations in Yunlin

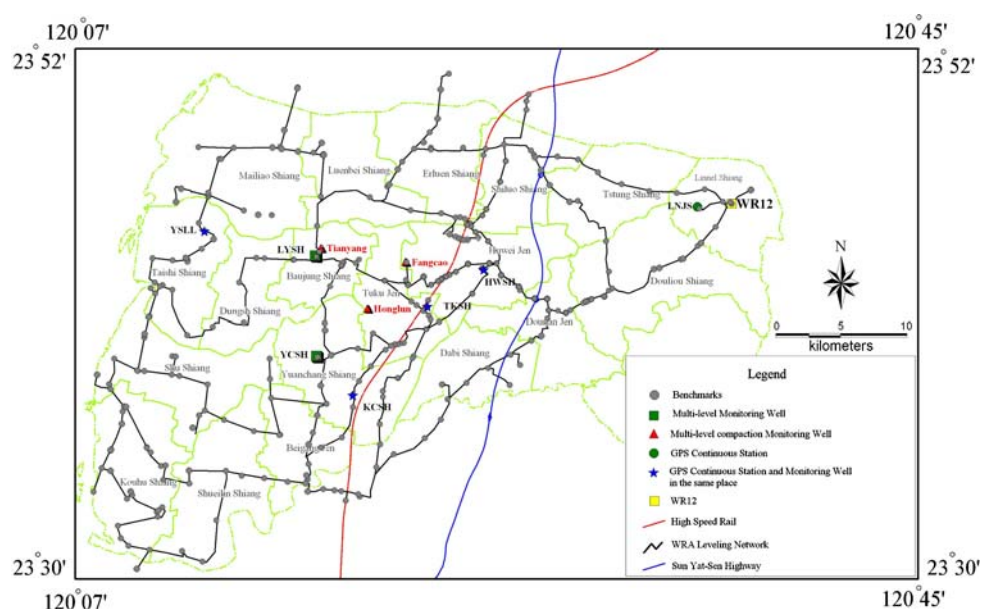


Table 2 Statistics of subsidence survey using leveling

Year	2000	2002	2003	2005	2006	2007
Length (km)	220	240	299	392	423	434
No. of observations	121	154	166	243	304	316
No. of benchmarks	117	150	161	232	292	303
Degree of freedom	5	5	6	12	13	14
A posteriori standard deviation (mm \sqrt{K})	0.60	0.57	0.69	0.60	0.80	0.79
Mean point error (mm)	3.3	3.5	3.7	3.0	3.5	3.4

Table 3 Maximum annual rate of subsidence and area of subsidence during 2002–07 in Yunlin

Year	2002	2003	2005	2006	2007
Max rate (cm/year)	9.5	12.2	11.6	10.1	8.2
Area with rate >3 cm/year (km ²)	610.5	703.1	678.6	557.1	551.5

outliers using Baarda’s data snooping method (Baarda 1968) and then least-squares adjusted to determine the heights of the benchmarks (Hwang et al. 2008). Table 2 summarizes the result of the adjustments for the leveling data collected in the five campaigns (2002–2007). The posteriori standard deviations of unit weight range from 0.5 to 0.8 mm \sqrt{K} , with a mean height standard error of 3 mm.

At any given benchmark, the height difference at two different epochs from leveling is its vertical displacement. In Yunlin, the vertical displacements from leveling are all negative, suggesting that subsidence occurs only in the study area (in eastern Taiwan, there exist large land uplifts due to the collision of the Philippine Sea Plate and the Eurasia Plate). The annual rates and areas of subsidence in different years are computed and shown in Table 3. The annual rate is defined as the ratio between the change in height and the time interval between successive campaigns. Contours of subsidence are computed using Kriging (Peng and Shih, 2002) and are shown in Fig. 7. Figure 8 shows the correlation between area of subsidence where subsidence exceeded 3 cm/year and rainfall. An annual subsidence rate of greater than 3 cm/year is considered significant and was used to determine the area of subsidence. In 2003, the subsidence area was the largest because a serious drought occurred in Taiwan that led to excessive pumping of groundwater and the largest subsidence area was measured this year. During 2005–2007, annual rainfall was near normal, resulting in less groundwater pumping and subsidence.

Monitoring of subsidence by multi-level compaction monitoring wells and continuous GPS

Leveling measures the integrated subsidence from land surface to the level of no subsidence. As shown in

Section “Introduction”, the subsurface deposits constituting the aquifer system in Yunlin are heterogeneous and contain layers of different hydraulic and mechanical properties. To better understand the mechanism of subsidence, it is critical to measure compaction at different stratigraphic intervals within the aquifer system. This can be achieved using a multi-level compaction monitoring well. As shown in Fig. 9, up to 26 magnetic rings are anchored at different depths in a borehole according to the stratigraphic variation. The depth of each magnetic ring was detected by a probe connected to a measuring tape made of indium-alloy with 1 mm accuracy. Four 300-m deep monitoring wells, named HWSH, TKSH, YCSH, and KCSH, have been installed in Yunlin (Fig. 6). Based on the stratigraphic types, 21–26 magnetic rings were anchored in each well (Table 4) and the depths of the rings were measured at a 1-month interval.

The change in the depth difference of two adjacent rings indicates the deformation of the stratigraphic section between the two rings; a shortening of the distance between the rings indicates compression or compaction of the stratigraphic section. On analyzing the changes of all the ring depths, the amount of each layer’s compaction to the total subsidence can be determined. In the CRAF, there are four strata with aquifers where groundwater can be withdrawn and thereby aquifer-system compaction might occur (Fig. 4). The compaction measured by the magnetic rings shows the extent of compaction in these four strata. For each stratum, the compaction per unit depth, defined as the ratio between the cumulative compaction measured in the stratum and the vertical length of the stratum, was then determined. The stratum with the maximum compaction per unit depth is defined as the major compaction stratum. Table 4 shows the major compaction stratum at the four monitoring wells.

Beyond the maximum depth of the well (300 m in this paper), compaction cannot be measured by the rings. Therefore, continuous GPS stations were established nearby at three of the compaction-monitoring wells (Fig. 6) to measure the total subsidence. Daily (24 h) coordinates at these GPS sites were determined. This daily sampling frequency by GPS is much higher than the yearly sampling

Fig. 7 Cumulative subsidence over 2002–2007 from leveling

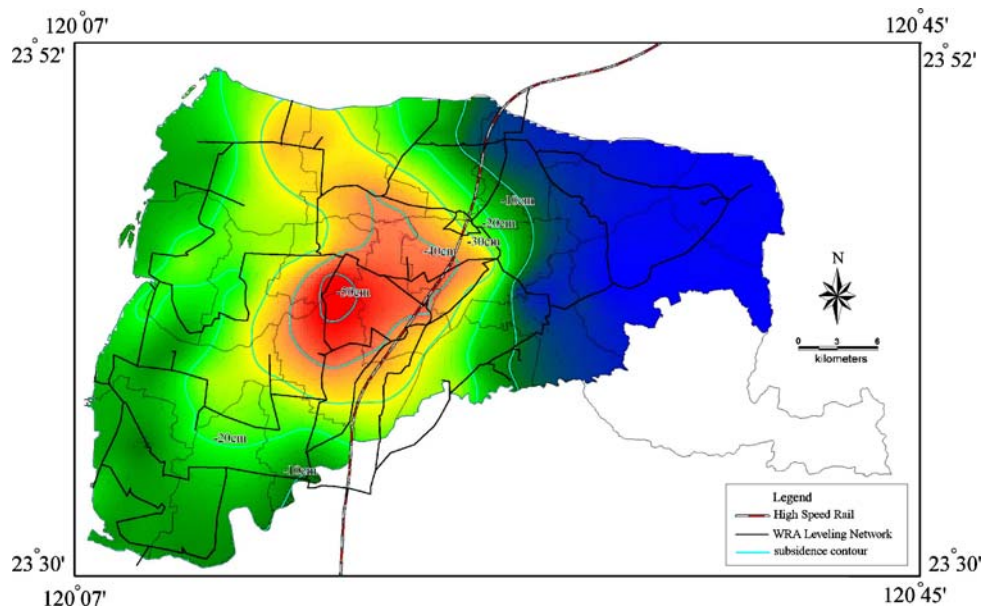
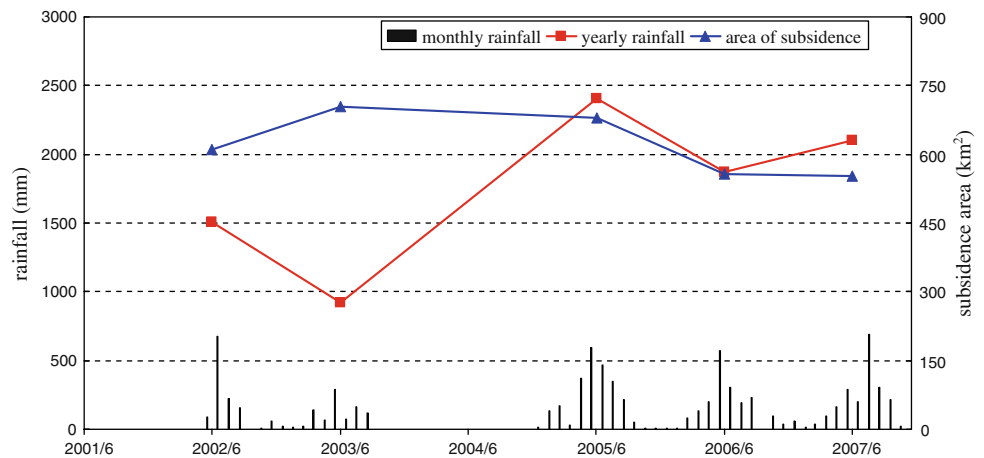


Fig. 8 Relationship between rainfall (both monthly and yearly) and area of subsidence where the annual rate of subsidence was greater than 3 cm/year. A yearly rainfall is given at the representative epoch of June of the year



frequency of leveling (Section “[Monitoring of subsidence by leveling](#)”). The GPS-derived subsidence can be used to validate the leveling result and to complement the compaction monitoring well data by determining the subsidence below the 300 m level.

Due to the GPS satellite geometry in general, the accuracy of GPS-derived vertical coordinate is three times worse than that of horizontal coordinates. Therefore, GPS data for subsidence needs to be processed carefully. According to UNAVCO (1999), there are five types of GPS pillar. Based on the geological settings in Yunlin and the obstruction condition of the GPS satellites near the compaction monitoring wells, a GPS pillar type with a concrete support was adopted. The construction of the GPS pillars used in this paper was detailed in Hung et al. (2000), and shown in Fig. 10. There are four such GPS pillars in Yunlin and three of them are co-located with the compaction monitoring wells (Fig. 6).

The GPS data processing and positioning were carried out using the Bernese 4.2 software developed by University of Bern (Beutler et al. 2001), Switzerland. The coordinates of the TNML station (Fig. 11), which belong to the International GPS Service (IGS) network, were held fixed in all GPS solutions. To ensure consistency with the international reference frame and Taiwan’s reference frame, a total of 20 continuous GPS stations were included in the GPS network solution and these stations are shown in Fig. 11. The stations outside of Yunlin are mostly continuous GPS tracking stations that define the coordinate frame of Taiwan.

Figure 12 compares the vertical displacements from leveling, GPS, and the compaction monitoring well at TKSH. All the vertical displacements are height differences referenced to the epoch in March 2006. The GPS result is based on the weekly averages of the daily solutions. Level surveys were done three times at TKSH (the reference point is WR12 in Fig. 6). The difference between

Fig. 9 A multi-level compaction monitoring well, **a** principle of measurement, **b** components, **c** in situ data collection

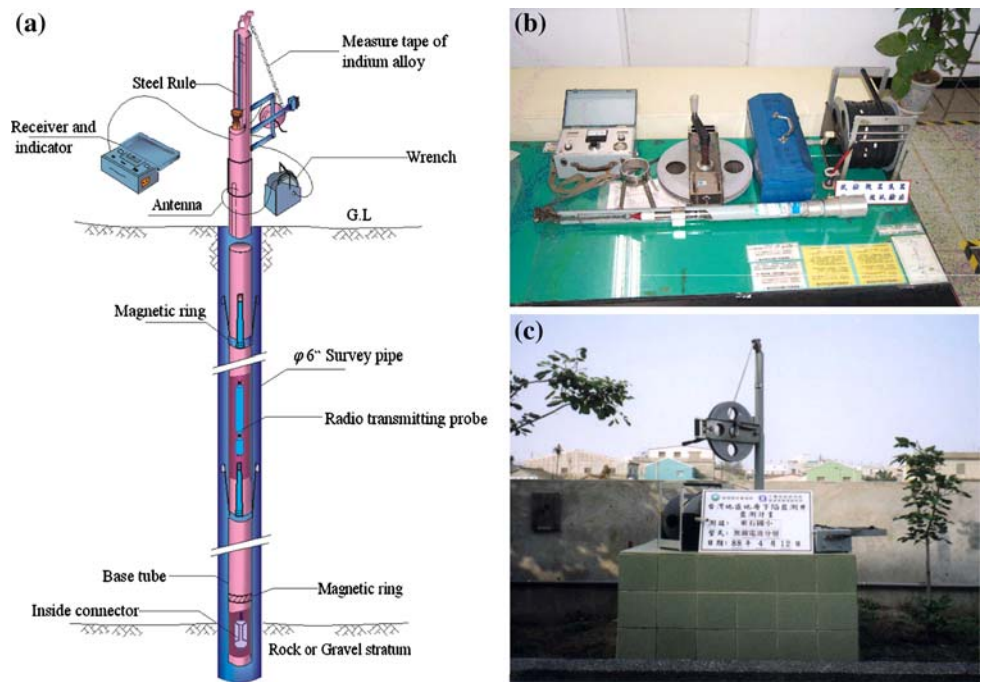


Table 4 A summary of compactions measured at four monitoring wells

Monitoring well	HWSH	TKSH	YCSH	KCSH
Depth (m)	300	300	300	300
No. of magnetic rings	26	26	26	21
Depth range of major compaction stratum (m)	270–300	240–300	250–300	250–300
Co-located with GPS	Yes	Yes	No	Yes

the GPS and leveling-derived displacements is a few mm, suggesting that GPS is an accurate tool for subsidence monitoring. However, the daily monitoring of subsidence by GPS delivers a temporal resolution unmatched by leveling. Figure 13 shows the yearly cumulative compaction profiles from 2004 to 2007 at the TKSH compaction monitoring well. A yearly cumulative compaction is the total compaction accumulated from the reference depth of 300 m to the land surface. In Fig. 13, the yearly cumulative compaction in 2004 is larger than subsequent years because ground withdrawal in Yunlin was regulated since 2005. The majority of compaction occurs at depths greater than 200 m, where the aquifer system contains highly compressible sand and clays. Because both GPS and leveling-derived displacements are larger than those derived from the compaction-monitoring well (Fig. 12), we conclude that aquifer system compaction also occurs at depths greater than 300 m. A majority of compaction at the HWSH and TKSH compaction-monitoring wells also occur at depths greater than 200 m and contribute more than 70% to the total compaction. The two wells are within few

hundreds of meters to THSR (Fig. 6). The compaction analysis in this paper suggests that, the regulation of groundwater withdrawal has significantly reduced compaction near THSR. Compaction at depths greater than 200 m were reduced from about 6 cm/year in 2004 to less than 3 cm/year in 2007 at TKSH. This suggests that further efforts to reduce the effects of groundwater pumping on the aquifer system at depths greater than 200 m could further reduce the subsidence-induced risk for THSR.

Spatially detailed monitoring of subsidence by differential radar interferometry

To apply the DInSAR technique, interferograms were produced from SAR (C-band) images acquired from the European Space Agency’s (ESA) ENVISAT satellite (launched in March 2002). DInSAR uses SAR-image pairs collected over a time interval to extract surface displacement by using the phase change of the radar signal in the direction of radar line-of-sight. The use of DInSAR for monitoring earth deformation process has received considerable attention because of its great potential for mapping the movement associated with earthquakes, volcano, and landslides (Zebker et al. 1994; Massonnet and Feigl 1998). DInSAR also has been applied to monitoring, analysis, and interpretation of land subsidence caused by aquifer-system compaction (for example, Galloway et al. 1998; Amelung et al. 1999; Hoffmann et al. 2001; Bell et al. 2002; Hoffmann et al. 2003; Galloway and Hoffmann 2007).

Fig. 10 The continuous GPS station near the TKSH monitoring well

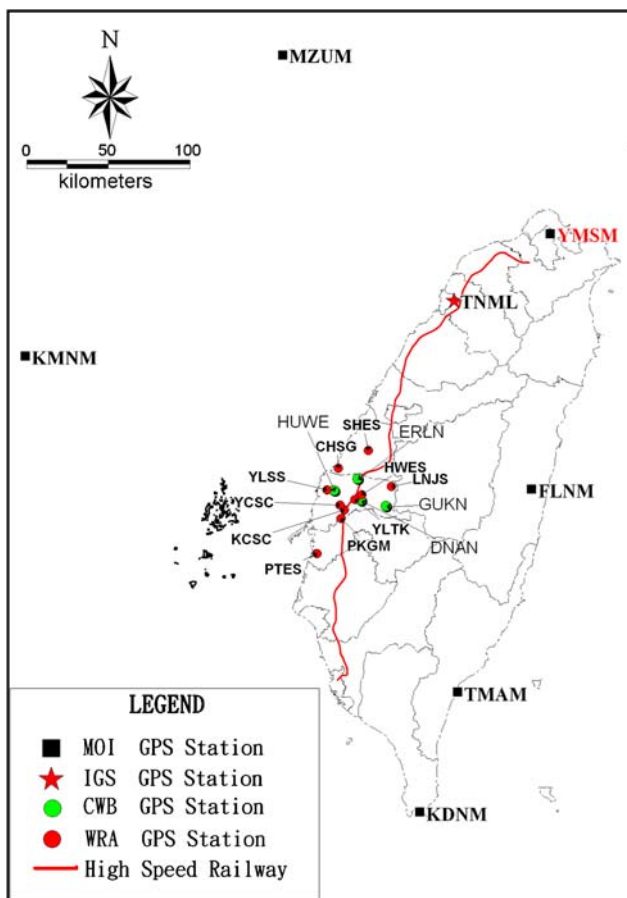
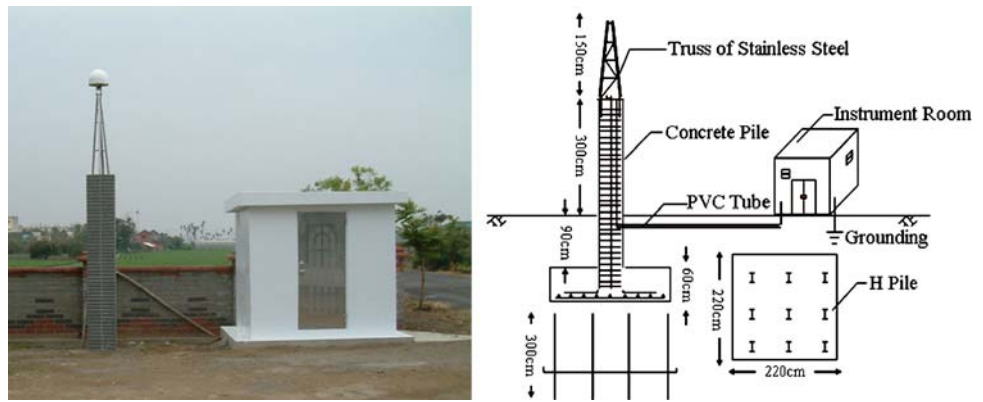


Fig. 11 Distribution of continuous GPS stations used for GPS solutions in Taiwan

Many factors affect the formation of an interferogram that is used to derive surface deformation. Two types of error can be most significant: orbital error and non-stationarity error (Pathier 2003). Orbital error will produce near-parallel fringes in an interferogram. In order to avoid this, precise orbits are needed. For this study, the precise orbits of ENVISAT computed at the Delft Institute for Earth-Oriented Space research (DEOS) of Delft University

of Technology (<http://www.deos.tudelft.nl/ers/precorbs/>) are used to account for the orbit error effect. The DEOS orbits are determined by sophisticated perturbing force models and satellite ranging and Doppler observations to the ENVISAT satellite, and reach an accuracy of better than 5 cm.

Two types of non-stationarity error exist. The first type of such error behaves like a random noise with a limited range. Examples of this type are errors from the digital elevation model (DEM), SAR processing, residual error caused by master and slave images, and error caused by the ground target. The second type of non-stationarity error is similar to ground surface deformation. Its distribution is not related to the characteristics of the ground target; instead, it is related to atmospheric conditions. Although radar can penetrate cloud and water vapor in the atmosphere, it will attenuate during the penetration. In some extreme weather conditions, for C-band radar atmosphere attenuation may lead to more than one fringe of error in the interferogram (Hoffmann 2003). In general, the atmospheric effect is not easily removed from the radar image and further limits DInSAR applications.

In order to reduce all possible errors, especially for the atmospheric error, we press as many image pairs as possible in this study. We chose eight images from the summer of 2006 to the summer of 2007 to generate 13 image pairs that have perpendicular baselines smaller than 400 m. The pairs of scenes that we used are listed in Table 5 and Fig. 14. We use the two-pass approach implemented by the Diapason software (Diapason 2006) to obtain the interferograms. In the resulting interferograms, the effects of topography were removed by using a 40×40 m DEM produced by the Taiwan Forestry Bureau. This DEM is retrieved from 1:5,000 topographic maps and its accuracy is about 1 m. We then estimated slant range displacement by using a phase unwrapping algorithm (Chen and Zebker 2002). Because the interferograms record only relative changes in phase, we cannot identify the position corresponding to no deformation as the starting point in the

Fig. 12 Comparison of vertical displacements from GPS (weekly averages from daily solutions), monitoring well and leveling (at TKSH)

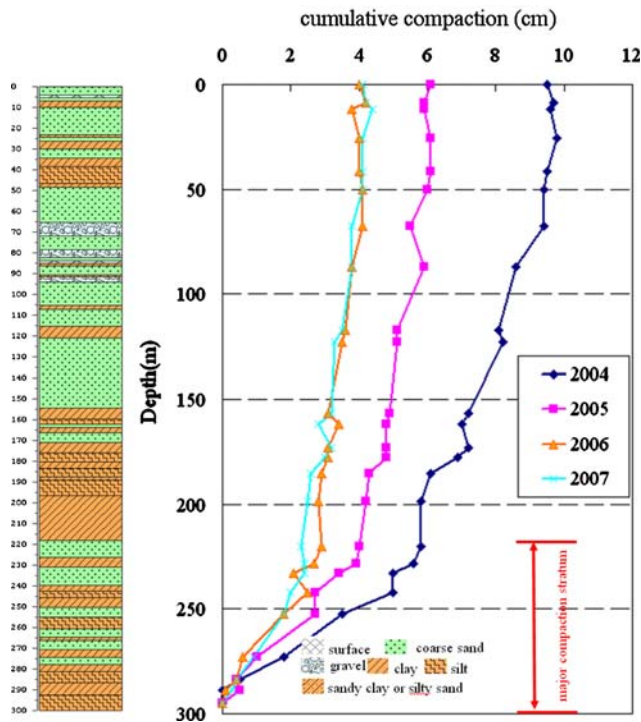
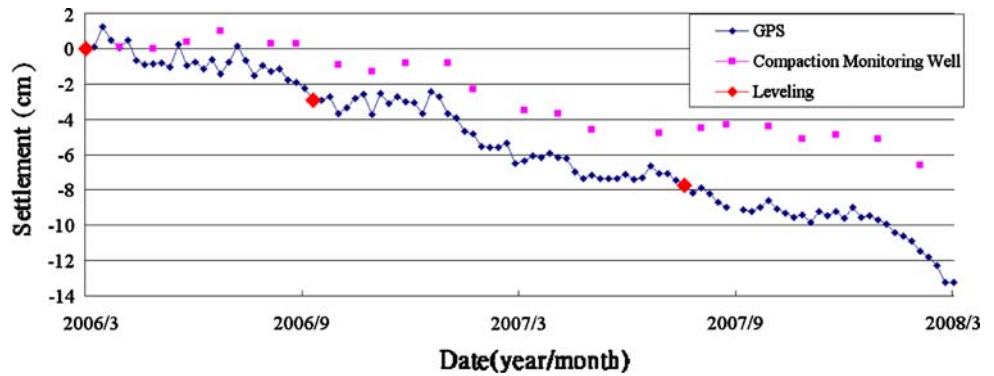


Fig. 13 Yearly cumulative compactions at the TKSH monitoring well. The column shows sediment types from surface (0 m) to the reference depth (300 m)

interferogram. Based on the results of leveling (Fig. 7), a reference point was chosen to carry out this unwrapping operation. Finally, the line-of-sight displacement fields (unwrapped interferograms) from the 13 image pairs were stacked to obtain average displacement rates over 2006–2007. The interferometric analysis provides only the range changes in the directions of line-of-sight between the radar and the ground, which vary from 19° in the near range area to 26° in the far range area. For consistency with the leveling data, the incident angles were used to convert the DInSAR line-of-sight results to vertical displacements (Fig. 15). Figure 16 shows vertical displacement rates interpolated from the point-wise leveling results (see Fig. 6 for the density of leveling benchmarks) over 2006–2007 in

Table 5 Parameters of ENVISAT SAR images: date of acquisition (y/m/d), vertical baseline offset (B_⊥) and interval time

Pair	Master image	Slave image	B _⊥	Days
1	2007/03/15	2007/01/04	130	70
2	2007/04/19	2007/02/08	141	70
3	2007/04/19	2007/03/15	190	35
4	2007/02/08	2006/10/26	306	105
5	2006/10/26	2006/09/21	362	35
6	2007/03/15	2007/02/08	331	35
7	2007/04/19	2007/01/04	320	105
8	2007/05/24	2007/02/08	88	105
9	2007/05/24	2007/03/15	243	70
10	2007/05/24	2007/04/19	53	35
11	2007/06/28	2007/02/08	58	140
12	2007/06/28	2007/03/15	273	105
13	2007/06/28	2007/04/19	83	70

Track = 232, frame = 3,123

Yunlin. The area covered in Fig. 16 was made roughly equal to that covered by DInSAR. Figure 15 (DInSAR) and Fig. 16 (leveling) show the largest subsidence near Tuku Township, and suggest that the subsidence in Yunlin is regional and possibly controlled by structural or stratigraphic-facies variations within the groundwater basin.

Figure 17 compares subsidence rates on the benchmarks along the AB and CD profiles (see Figs. 15, 16) from DInSAR and leveling. The RMS differences are 1.2 and 1.1 cm along AB and CD, respectively. The DInSAR result is the averaged vertical displacement rate from October 2006 to July 2007, while the leveling-derived result is the averaged rate from October 2006 to August 2007. The slightly different time intervals may be a source of the discrepancy. Furthermore, a careful comparison of the results in Fig. 15 (DInSAR) and Fig. 16 (leveling) reveals that many minor and locally distributed displacements obtained by DInSAR are not detected by leveling. This shows the strength of DInSAR in enhancing the spatial resolution of subsidence monitoring. Despite problems such as spatial de-correlation, orbit error, ionospheric long-

Fig. 14 ENVISAT SAR data used in this study. Cross axle shows the time and the vertical axle shows the vertical baseline offset of each image pair. Track = 232, frame = 3123

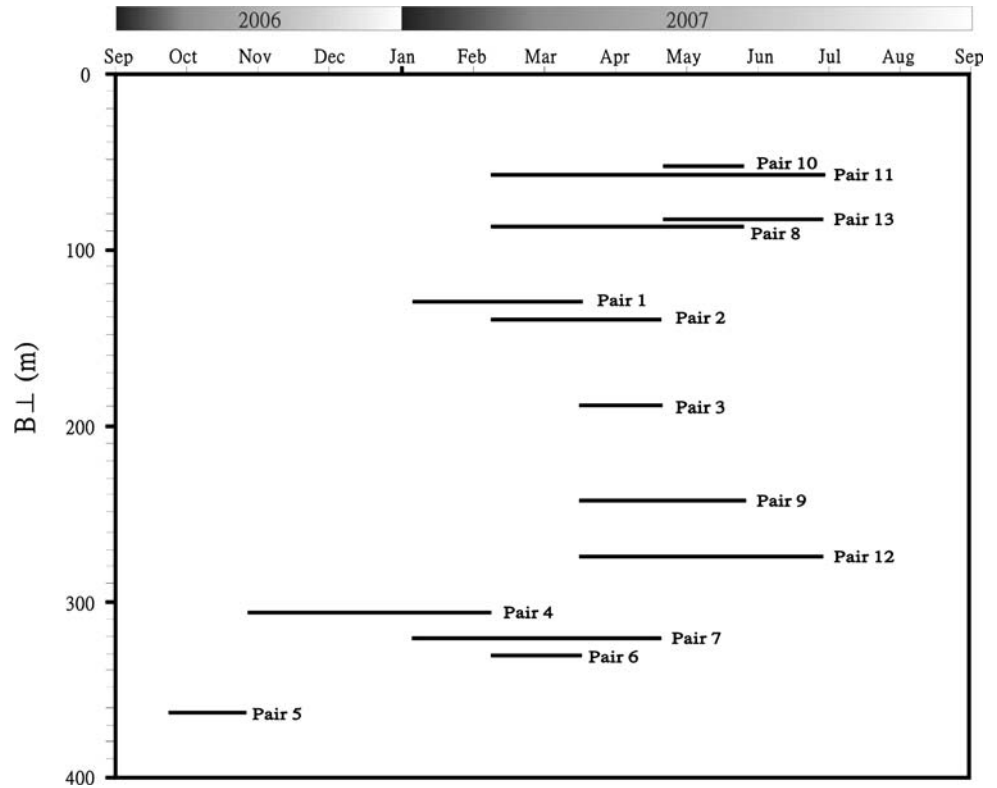
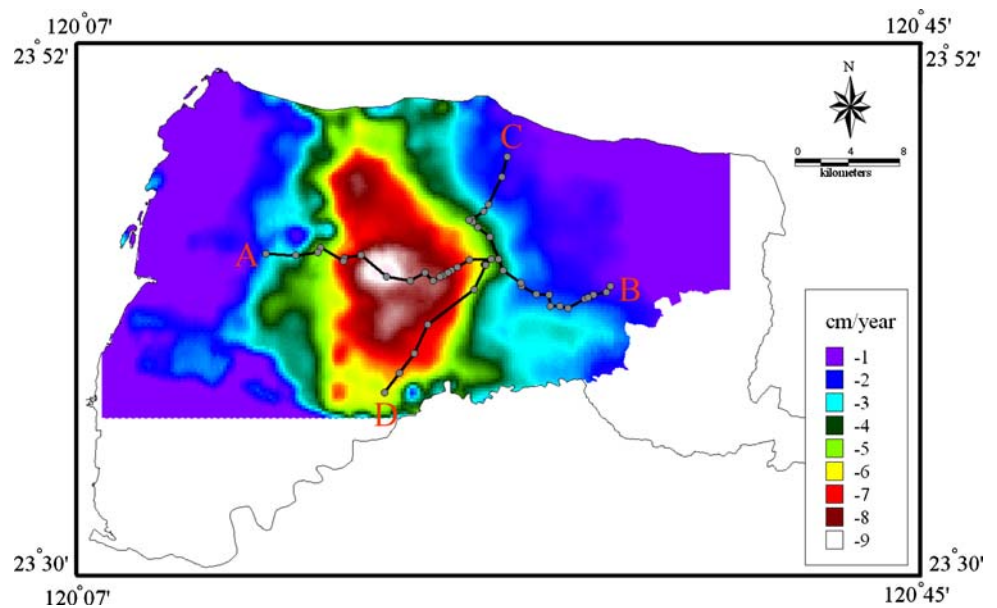


Fig. 15 Vertical displacement rate derived from DInSAR result over 2006–2007. Circles along lines AB and CD are leveling benchmarks used in Fig. 16



wavelength disturbance or tropospheric gradients in moisture, DInSAR proved a useful and high-resolution tool for detecting surface deformation in Yunlin.

Discussion and conclusions

In this study, leveling, GPS, compaction monitoring wells, and DInSAR are used to detect subsidence in the

CRAF. The results from these sensors are consistent in accuracy and complementary in their spatial and temporal resolutions. The result obtained here is vital for the Taiwan government in the issue of subsidence mitigation in Yunlin.

The leveling result points out that in 2007 the area of subsidence (rate >3 cm/year) in Yunlin is about 551.5 km² with a maximum rate of 8.2 cm/year. The result of compaction monitoring wells shows that about 70% of

Fig. 16 Vertical displacement rate obtained by leveling result over 2006–2007. Circles are the same as those in Fig. 15

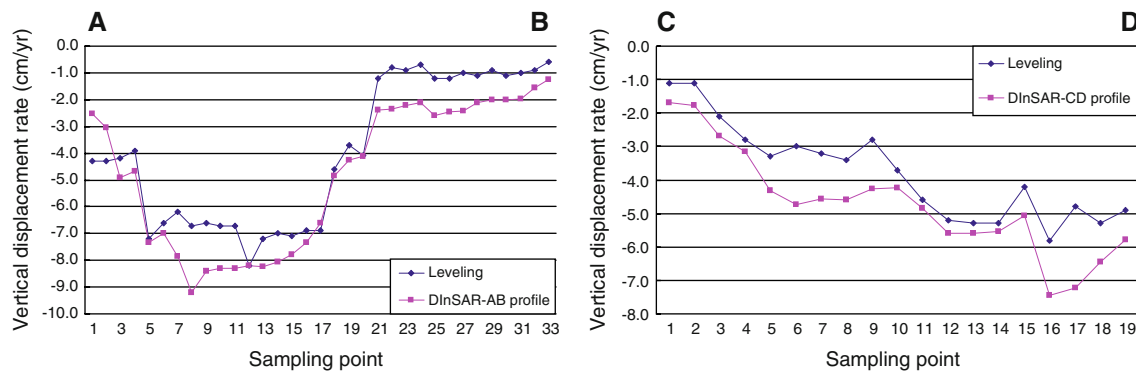
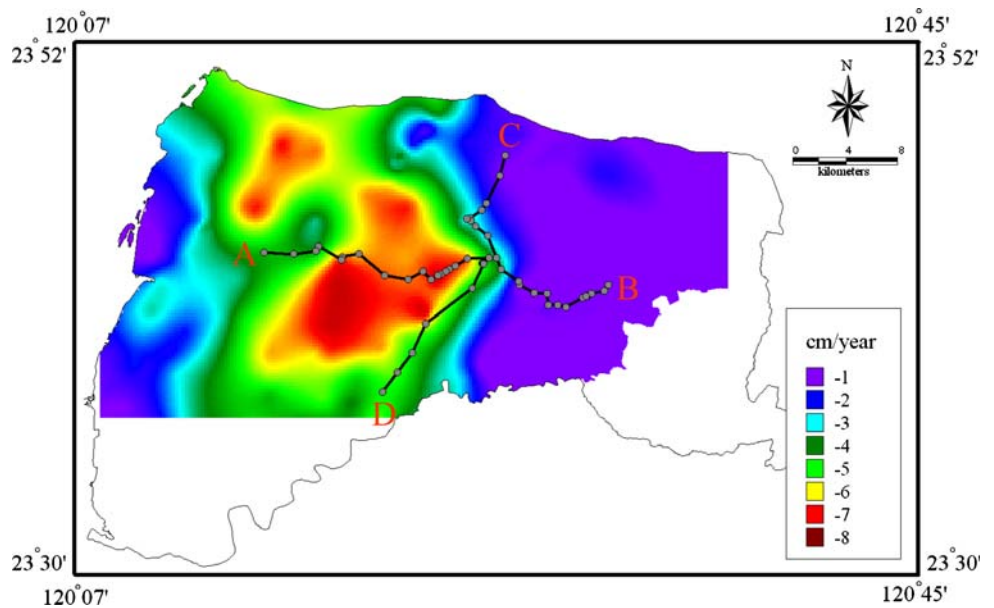


Fig. 17 Vertical displacement rates over 2006–2007 from leveling and DInSAR on leveling benchmarks along AB and CD

subsidence occurs at depths below 200 m along the rail of THSR in Yunlin. If such subsidence will affect the safety of THSR, groundwater pumping here should be strictly controlled. Both GPS and leveling-derived vertical displacements at the compaction monitoring wells are larger than those from the wells, indicating that subsidence also occurs below 300 m (the depth of the wells).

The main disadvantage of leveling and GPS is that they can only detect point-wise deformations. If spatially detailed deformation is needed, it will require a large amount of leveling and GPS pillars, and frequent visits, which demands a large budget. This disadvantage is compensated by DInSAR, which uses SAR images to map deformation at a high spatial and temporal resolution (25 m and 35 days for ENVISAT). The subsidence measured using DInSAR in this study matches that from leveling to 1–2 cm, confirming DInSAR is a competent tool in subsidence detection. However, many potential errors may degrade the DInSAR results (Section [Spatially detailed](#)

[monitoring of subsidence by differential radar interferometry](#)). In particular, Yunlin is covered by different vegetations over different seasons so that spatial de-correlation might lead to a degraded or incorrect deformation result. This problem can be reduced by the PS-InSAR technique (Ferretti et al. 2001; Hooper et al. 2007) or the SBAS technique (Berardino et al. 2002), and this is a subject of future study.

Acknowledgments This study is supported by the National Science Council (Project number: 96-2221-E-009-165) and the Water Resource Agency, Dept of Economics, Taiwan, ROC.

References

Amelung F, Galloway DL, Bell JW, Zebker H (1999) Sensing the ups and downs of Las Vegas: InSAR reveals structural control of land subsidence and aquifer-system deformation. *Geology* 27(6):483–486

- Baarda W (1968) A testing procedure for use in geodetic networks. Netherlands Geodetic Commission. Publ. on Geodesy, 2(5), Delft
- Bell JW, Amelung F, Ramelli AR, Blewitt G (2002) Land subsidence in Las Vegas, Nevada, 1935–2000: new geodetic data show evolution, revised spatial patterns, and reduced rates. *Environ Eng Geosci* 8(3):155–174
- Berardino P, Fornaro G, Lanari R, Sansosti E (2002) A new algorithm for surface deformation monitoring based on small baseline differential SAR interferograms. *IEEE Trans Geosci Remote Sens* 40(11):2375–2383
- Beutler G, Brockmann E, Dach T, Fridez P, Gurtner W, Hugentobler U, Johnson J, Mervart L, Rothacher M, Schaer S, Springer T, Weber R (2001) Bernese GPS Software Version 4.2, Astronomical Institute, University of Berne, Bern, p 515
- Central Geological Survey of Taiwan (CGS) (1999) The investigation of hydrogeology in the Choshui River alluvial fan. CGS Publications, Taipei, p 130 (in Chinese)
- Chen CW, Zebker HA (2002) Phase unwrapping for large SAR interferograms: statistical segmentation and generalized network models. *IEEE Trans Geosci Remote Sens* 40:1709–1719
- Diapason (2006) Automated interferometric processing software version 4.0, Altamira Information, France
- Ferretti A, Prati C, Rocca F (2001) Permanent scatterers in SAR interferometry. *IEEE Trans Geosci Remote Sens* 1(39):8–20
- Galloway DL, Hoffmann Jörn (2007) The application of satellite differential SAR interferometry-derived ground displacements in hydrogeology. *Hydrogeol J* 15(1):133–154. doi:10.1007/s10040-006-0121-5
- Galloway DL, Hudnut KW, Ingebritsen SE, Phillips SP, Peltzer G, Rogez F, Rosen PA (1998) Detection of aquifer-system compaction and land subsidence using interferometric synthetic aperture radar, Antelope Valley, Mojave Desert, California. *Water Resour Res* 34:2573–2585
- Galloway D, Jones DR, Ingebritsen SE (1999) Land subsidence in the United States. Reston, Virginia, p 177
- Hasanuddin ZA, Djaja R, Darmawan D, Hadi S, Akbar A, Rajiyowiryo H, Sudibyo Y, Meilano I, Kasuma MA, Jahar J, Subarya C (2001) Land Subsidence of Jakarta (Indonesia) and its Geodetic Monitoring System. *Nat Hazards* 23:365–387
- Hoffmann J (2003) The application of satellite radar interferometry to the study of land subsidence over developed aquifer systems. PhD thesis, Stanford University
- Hoffmann J, Galloway DL, Zebker HA, Amelung F (2001) Seasonal subsidence and rebound in Las Vegas Valley, Nevada, observed by synthetic aperture radar interferometry. *Water Resour Res* 37:1551–1566
- Hoffmann J, Galloway DL, Zebker HA (2003) Inverse modeling of interbed storage parameters using land subsidence observations, Antelope Valley, California. *Water Resour Res* 39(2):1031. doi:10.1029/2001WR001252
- Hooper AZ, Howard SP, Kampes B (2004) A new method for measuring deformation on volcanoes and other natural terrains using InSAR persistent scatterers. *Geophys Res Lett* 31:23611. doi:10.1029/2004GL021737
- Hooper A, Segall P, Zebker H (2007) Persistent scatterer interferometric synthetic aperture radar for crustal deformation analysis, with application to Volca'n Alcedo, Gala'pagos. *J Geophys Res* 112. doi:10.1029/2006JB004763
- Hung WC (2007) Taiwan land subsidence monitoring and surveying analysis, Report of Industrial Technology Research Institute (ITRI), Hsinchu (in Chinese)
- Hung WC, Peng MH, Liu JK (2000) The result of installing a GPS continuous station. In: Proceedings of the 19th survey symposium, Taiwan (in Chinese), pp 84–93
- Hwang C, Hsiao YS (2003) Orthometric correction from leveling, gravity, density and elevation data: a case study in Taiwan. *J Geod* 77:279–291
- Hwang C, Hung WC, Liu CH (2008) Results of geodetic and geotechnical monitoring of subsidence for Taiwan High Speed Rail operation. *Nat Hazards*. doi:10.1007/s11069-007-9211-5
- Lin LH, Lin HR, Ke AHW, Chou TH (1992) Petroleum potential of the Pre-Miocene Formations in the Chianan Plain, Taiwan. *Petrol Geol Taiwan* 27:177–197
- Liu CW, Lin WS, Shang C, Liu SH (2001) The effect of clay dehydration on land subsidence in the Yun-Lin coastal area, Taiwan. *Environ Geol* 40(4/5):518–527
- Marfai MA, King L (2007) Monitoring land subsidence in Semarang, Indonesia. *Environ Geol* 53:651–659
- Massonnet D, Feigl KL (1998) Radar interferometry and its application to changes in the Earth's surface. *Rev Geophys* 36:441–500
- Pathier E (2003) Apports de l'interférométrie radar différentielle à l'étude de la tectonique active de Taiwan. PhD thesis, Univ. Paris VI. Paris, France, p 273
- Peng MH, Shih TY (2002) A quality assurance approach for land subsidence interpolation. *Survey Rev* 36(286):568–581
- Pietro LT, Laura T, Frankenfield CJ (2007) A new project to monitor land subsidence in the northern Venice coastland (Italy). *Environ Geol* 52:889–898
- Population Division, Department of Economic and Social Affairs, United Nations (2005). World Population Prospects: The 2004 Revision. United Nations
- Tyan CL, Chang YM, Lin WK, Tsai MK (1996) The brief introduction to the groundwater hydrology of Choshui River alluvial fan. In: Proceeding of groundwater and hydrogeology conference in Choshui River Alluvial Fan, Taipei, Taiwan (in Chinese), pp 207–221
- UNAVCO (University NAVASTAR Consortium) (1999). In Continuous Station Equipment\Monumentation from <http://unavco/www.unavco.ucar.edu/index.htm>
- Zebker HA, Rosen PA, Goldstein RM, Gabriel A, Werner CL (1994) On the derivation of coseismic displacement fields using differential radar interferometry: the Landers earthquake. *J Geophys Res* 99(19):617–619 634